ORIGINAL ARTICLE

WILEY

Aging-induced atrial fibrosis in I_f current change and its effect on atrial fibrillation in dogs

Fei-Fei Wang MD[1,2,3] | **Ya-Fan Han MD**[1,2] | **Xiao-Yan Liang PhD**[1,2] | **Ge-Ge Zhang PhD**[1,2] | **Yan-Mei Lu PhD**[1,2] | **Yao-Dong Li PhD**[1,2] | **Bao-Peng Tang PhD**[1,2]

[1]Department of Pacing and Electrophysiology, The First Affiliated Hospital of Xinjiang Medical University, Urumqi, China

[2]Xinjiang Key Laboratory of Cardiac Electrophysiology and Cardiac Remodeling, The First Affiliated Hospital of Xinjiang Medical University, Urumqi, China

[3]Xinjiang Emergency Center, People's Hospital of Xinjiang Uygur Autonomous Region, Xinjiang, China

Correspondence
Yao-Dong Li and Bao-Peng Tang, Department of Pacing and Electrophysiology, The First Affiliated Hospital of Xinjiang Medical University, No. 137 South liyushan Road, Xinshi District, 830000 Urumqi, Xinjiang, China.
Emails: liyaodong_123@outlook.com (Y-DL); tangbaopeng0923@163.com (B-PT)

Abstract

Background: Atrial fibrillation (AF) is a very common type of cardiac arrhythmia that threatens public health. Aging is an independent AF risk factor. However, the mechanism of age-related AF remains unclear.

Methods: A total of 36 Beagle dogs were selected and divided into three groups (12 in each group): two groups were 9-year-old aged dogs, and one group was 4-year-old adult dogs. Electrophysiological testing was employed to determine if modeling is successful. Patch-clamp technique was employed to measure the I_f current. The expression of protein and mRNA related to I_f current were also tested. Collagen deposition was observed with the use of Masson staining.

Results: Aging resulted in a higher collagen deposition percentage in the left atrium. The hyperpolarization-activated cyclic nucleotide-gated (HCN)2 and HCN4 expressions were increased in the atria and pulmonary veins but decreased in the sinus node of the aged group. Moreover, in the aged group, the left atrium mRNA expressions of Kcnd2 (Potassium voltage-gated channel subfamily D member 2), Kcnh2, Kcnq1, Kcnj2, Kcnj11, and CACNA1H were significantly downregulated. The aged AF group also demonstrated sustained AF and significant changes in electrophysiological characteristics. The I_f current demonstrated an increased amplitude and was easier to activate in the aged AF group than in younger group. Finally, AF occurrence exacerbated aging-induced cardiac fibrosis, thereby aggravating the above-listed symptoms.

Conclusion: With age, the increase in atrial fibrosis affected the expression of the ion channels, thereby modulating the I_f current. Moreover, AF also further exacerbated the degree of atrial fibrosis.

KEYWORDS
abnormal current, age-related atrial fibrillation, I_f current, left atrial fibrosis

---

Fei-Fei Wang and Ya-Fan Han contributed equally to this study.

-----

1 | INTRODUCTION

Atrial fibrillation (AF) is a highly prevalent type of arrhythmia threatening public health. In Europe, 120,000–15,000 new cases of AF are being reported every year (Kirchhof et al., 2017). AF contributes to the onset of stroke, heart failure, sudden death, and other life-threatening conditions (Oldgren et al., 2014; Thihalolipavan & Morin, 2015; Zoni-Berisso et al., 2014). Aging is an independent AF risk factor (Cremer et al., 2015); this might contribute to the high AF prevalence in the aged population, making the above-listed conditions even more dangerous than the younger group. However, the mechanism of age-related AF remains unclear.

Cardiac fibrosis is a chronic pathological change closely related to age (Babür Güler et al., 2011). Atrial fibrosis usually contributes to increased myocardial stiffness, myocardial hypertrophy, and ventricular dilatation (Babür Güler et al., 2011). In addition, cardiac diseases caused by myocardial fibrosis usually result in decreased ejection fraction and changes in electrophysiological characteristics (Gyöngyösi et al., 2017), eventually reducing cardiac function. Myocardial fibrosis is generally caused by inflammation and myocardial damage (Espeland et al., 2018); however, recent studies have found that aging also contributes to the development of myocardial fibrosis (Jiang et al., 2017), one of the main factors leading to cardiac remodeling in patients with AF. However, the aging-induced effects of myocardial fibrosis on AF and its related mechanism remain unclear.

Hyperpolarization-activated cyclic nucleotide-gated (HCN) channels are ion channels important for automatic depolarization in phase IV (Benarroch, 2013). The funny current (I_f) is an inward Na^+/K^+ current governed by 4 HCN subtypes (HCN1-4) (Rivolta et al., 2020). HCN1-4 mainly exists in the sinus node. On one hand, it plays an important role in the regulation of sinus node pacing. On the other hand, HCN1-4 cardiomyocyte expression in the atrium and other working myocardia may become an ectopic pacemaker and contribute to the development of AF.

Aging is the main cause of degenerative heart changes (Love & Miners, 2016). Recent studies have found that aging will reduce the pacing function in the sinus node and ultimately lead to AF occurrence (Hirosawa et al., 1987). However, the sinus node HCN expression, AF occurring in the central atrium and pulmonary veins during aging, and I_f changes have not been well studied.

In the present study, a canine aging AF model was established to examine the relationship between AF and cardiac fibrosis, as well as achieve a preliminary understanding of the related underlying mechanisms.

2 | MATERIALS AND METHODS

2.1 | Animals

The study protocol was approved by the ethics committee of the First Affiliated Hospital of Xinjiang Medical University (NO. IACUC201902-k05), and the guidelines for animal experiments issued by the First Affiliated Hospital of Xinjiang Medical University were followed strictly in animal care and feeding procedures.

A total of 36 beagle dogs weighing 16–20 kg were randomly assigned to three groups: the adult sinus rhythm group (aged 4 years; $n = 12$), the aged sinus rhythm group (aged 9 years; $n = 12$), and the aged AF group (aged 9 years; $n = 12$). The animals were anesthetized with pentobarbital sodium before surgery, and atrial pacing electrodes were implanted into the atria without X-ray through the external jugular vein to obtain 600 times/min rapid pacing. We used pacemaker AOO mode high-frequency pacing (600 beats/minute for 8 weeks) to induce the atrial fibrillation. The successful pacing identification was that in the ECG mode, and the p wave disappeared with the ECG characteristics of F waves. And the rhythm is absolutely uneven, the strength of different signs. The above phenomenon appears in model dogs that we call mold-making success. This is a continuous study, and we will take cardiac electrophysiological detection and patch clamp for further research. The intervention lasted 8 weeks. Subsequently, if AF was maintained for 15 min after the intervention was stopped, it indicated that the AF model was successfully established.

2.2 | Cardiac ultrasound testing

Echocardiography was performed before and 8 weeks after the operation in each animal, and the data on ejection fraction, end-diastolic and systolic left ventricle diameters and left and right atrial diameters were collected. At the same time, the presence of valvular disease or congenital heart disease was investigated, and unqualified subjects were disqualified from the study. We found no beagles with congenital heart disease and valvular disease.

2.3 | Electrophysiological testing

The electrocardiographic tests were performed on the atria and pulmonary veins using a multiple lead system. The sinus node function was assessed through the observation of sinus node recovery using corrected sinus node recovery time (SNRTc). A two-fold diastolic threshold and 250 ms S1–S1 interval were used to stimulate the high right atrium for 30 s. The SNRTc was defined as the time between the last stimulus-induced atrial A wave and the first sinus A wave minus the time between the first sinus A wave and the second sinus A wave. The effective refractory period (ERP) of each site was measured by 300 ms S1–S2 interval stimuli and the stimulation voltage was 2 × the diastolic threshold. ERP was defined as the longest S1–S2 interval in the S1S2; it could not effectively recover under the 300 ms stimulation duration. ERP dispersion (ERPd) was defined as the difference between the longest ERP and the shortest ERP, including intracardiac ERPd (AERPd) and the pulmonary vein ERPd (PVERPd). ERP frequency adaption was defined as the change of ERP under programmed stimulation with a different stimulation parameter in the same mapping site, with (ERP300−ERP150)/50 ms as the evaluation index of ERP frequency adaption. The mapping sites included the pulmonary vein, left and right atria, and proximal and distal coronary veins.

2.4 | Cell separation and whole-cell patch-clamp recording

A total of 5 dogs from each group underwent patch-clamp recording; a minimum of three cells were recorded for the I_f current. Cardiomyocytes were isolated using the Langendorff perfusion device. In summary, the dog's chest was opened and the heart quickly removed under anesthesia with 3% pentobarbital sodium (30 mg/kg). The heart was placed in a balanced salt solution containing 15 mM potassium chloride. The heart was placed on the Langendorff device and perfused for 30 ml/min with a balanced, calcium-free, and enzyme-containing salt solution. The perfusion was maintained for 60 min after the heart was entirely filled until the digestion was complete. The resulting single, rod-like cells were used for patch-clamp recording. The liquid oxygen content was 80%–90% in all cases, and the experiment was performed at room temperature.

The whole-cell patch-clamp recording was conducted using the Heak EPC10 amplifier; the recording electrode had a resistance of 4–6 MΩ. The pipette solution contained: K-glutamate (130 mmol/L); KCl (15 mmol/L); NaCl (5 mmol/L); MgCl$_2$ (1 mmol/L); HEPES (10 mmol/L); EGTA (2 mmol/L); and MgATP (5 mmol/L) (pH 7.2, KOH). The extracellular fluid contained: NaCl (137 mmol/L); KCl (5.4 mmol/L); CaCl$_2$ (1.8 mmol/L); MgCl$_2$ (1 mmol/L); BaCl$_2$ (1 mmol/L); HEPES (5 mmol/L); and glucose (10 mmol/L) (pH 7.4, NaOH). A standard cell-attached method was used to form a high-impedance seal, with a cell-sealing resistance of >2 GΩ. Fast capacitance was compensated for, and the cell membrane was ruptured to achieve whole-cell recording. After this, the slow capacitance compensation and series compensation were adjusted to reduce the instantaneous discharge current and clamping error. The I_f currents were recorded by holding the resting membrane potential at −40 mV; the stimulus voltage ranged from −160 to −40 mV, with intervals of 20 mV, and was maintained for 2000 ms to induce the hyperpolarization-activated inward current. Each test potential was followed by a step to −160 mV for 1 s to examine its activation kinetics; it was then brought to the holding potential of −40 mV.

2.5 | Real-time polymerase chain reaction

Left atrial tissue was used, and total RNA was extracted from the tissue with the use of the RNA extraction kit (Tiangen). The process was conducted according to the manufacturer's instructions as well as the messenger RNA (mRNA) sequence of target HCN2 and HCN4 in GenBank. The primers were designed by premier 5.0 software (Table 1). The complementary DNA templates were subjected to a serial dilution of 10, 10^2, 10^3, 10^4, 10^5, and 10^6, and were analyzed using fluorescence quantitative polymerase chain reaction (PCR). The amplification efficiency of the primers was 0.9–1.1. At the same time, the primer (10 μM) was subjected to fluorescence quantitative PCR analysis. A melting curve analysis at 95–65°C was performed after the end of the reaction (Table 1).

TABLE 1 The primers in this study

Gene	Primers
CACNA1H	(F): 5′-TTCGTCTTCTTCATCTTCGGCATCG–3′ (R): 5′-CCGCAGGAAGGTGAGGTTGTTG–3′
KCNJ11	(F): 5′-GCCCACCATCCAGACTTGAACTC–3′ (R): 5′-TAGCAGCCCAAAGACCCTCCAC–3′
Kcnj2	(F): 5′-CCAACCGCTACAGCATCGTCTC–3′ (R): 5′-CCTTACTCTTCCCGTTCCCAAAGC–3′
Kcnq1	(F): 5′-TCATCGTCCTGGTCTGCCTCATC–3′ (R): 5′-CCACATACTCCGTCCCAAAGAACAC–3′
Kcnh2	(F): 5′-GTGGTGGACTTCATCGTGGACATC–3′ (R): 5′-TCGTTGGCATTGACATAGGTGGTG–3′
KCND2	(F): 5′-ATGAGTTTGTGGATGAGCAGGTCTTC–3′ (R): 5′-TGTGTCGTCGTGAACAGCAAGTG–3′
TGFB1	(F): 5′-CATGGCATGAACCGACCCTTCC–3′ (R): 5′-CCGTGGAGCTGAAGCAGTAGTT–3′
MMP2	(F): 5′-CCGTCGCCCATCATCAAGTTCC–3′ (R): 5′-CAGCCGTAGTAGGTGTTCAGGTATTG–3′
FN1	(F): 5′-TGGATGATGGTGGATTGTACTTGTCTG–3′ (R): 5′-CTTCTTGCTCCAGGTATCTCCGATTC–3′
Col3a1	(F): 5′-GACCTGGTTGCTTCTCGCTCTG–3′ (R): 5′-ATTTGGCACGGTTCTGGCTTCC–3′
Col1a1	(F): 5′-CCTGAAGGAAGCCGCAAGAACC–3′ (R): 5′-GGTCAATCCAGTATTCTCCGCTCTTC–3′
GAPDH	(F): 5′-CCTGCACCACCAACTGCTTG–3′ (R): 5′-ATGGCATGGACGGTGGTCAT–3′

2.6 | Western blot

The total protein of left atrial tissue was extracted after tissue lysis with Western and IP lysate (Beyotime). After the protein was quantified using the bovine serum albumin kit (Beyotime), 20 μg of protein was boiled with loading buffer and subjected to 12% polyacrylamide gel electrophoresis. The protein was then transferred to the nitrocellulose membrane (Millipore, UK) and blocked with 5% skimmed milk at 4°C overnight. Then, appropriately diluted primary antibodies (HCN2 [Bioss]: 1:500; HCN4 [Bioss]: 1: 250; glyceraldehyde 3-phosphate dehydrogenase [GAPDH] [Santa Cruz]: 1: 500) were added and incubated at room temperature for 2 h. After washing the membrane with 1 × tris buffered saline with tween (TBST) for 10 min three times, the corresponding secondary antibody HRP Conjugated Rabbit Anti-Goat IgG (H + L) [A21030; Abbkine; 1:1000] was added and incubated at room temperature for 1 h. The membrane was then again subjected to washing with 1 × TBST for 10 min three times. Efficient chemiluminescence (ECL) chemiluminescent substrate (Millipore) was prepared, and the ChemiDoc-It HR 410 imaging system (Upland, CA) was used to analyze the results.

2.7 | Masson staining

The paraffin section of left atrial samples from 3 dogs in each group was dewaxed, and the samples were subjected to staining and

washing with the Masson's Trichrome Stain Kit (Solarbio). The samples were observed under a microscope; the images were analyzed using a medical pathology color image analyzer, and the collagen volume fraction was calculated.

2.8 | Statistical analysis

All data were expressed as the mean ± standard deviation. Differences between two groups were analyzed using the Student's *t*-test, while differences among three groups were analyzed using one-way Analysis of Variance. The rank-sum test was applied if the data did not fit a normal distribution. The Western blot data included the gray value after imaging, and the patch-clamp data included the mean current of each point. A *p* value of <.05 was considered statistically significant in the two-tailed test.

3 | RESULTS

### 3.1 | Aging and AF cause left atrial fibrosis in dogs

To study the effect of aging on left atrial fibrosis, the Masson staining was used to detect the expression of collagen in adult and aged dogs. The results showed that collagen fibers accounted for 21.96%, 47.86%, and 60.24% of the left atrium tissue in the adult dog group, the elderly dog group, and the atrial fibrillation elderly dog group, respectively(Figure 1a,b). Moreover, RT-PCR results showed that the mRNA expression of Col1a1, Col3a1, FN1, MMP2, MMP9, and Tgfb1 in the left atrium tissue of the elderly dog group and the AF elderly dog group were significantly increased compared with the adult dog group (Figure 2a–f).

3.2 | Aging and AF changes heart structure and reduces heart function in dogs

In order to further study the effect of aging on atrial, changes in heart function were detected. The results showed no significant differences in the ejection fraction, left atrium diameter, right atrium diameter, and left ventricular end-diastolic and end-systolic diameters between the aged group and the adult group (Figure 3a,c). Moreover, compared with the AF elderly dog group, the left atrium diameter in the elderly dog group decreased significantly, while the ejection fraction increased significantly (Figure 3b,c). The above results indicate that AF contributed to cardiac function change and heart structure remodeling.

3.3 | Aging and AF reduce canine heart ERP

In order to further study the effects of aging and AF on cardiac function, the ERP was detected. The results showed that compared to the adult dog group, AERPd, PVERPd, and SNRT were significantly
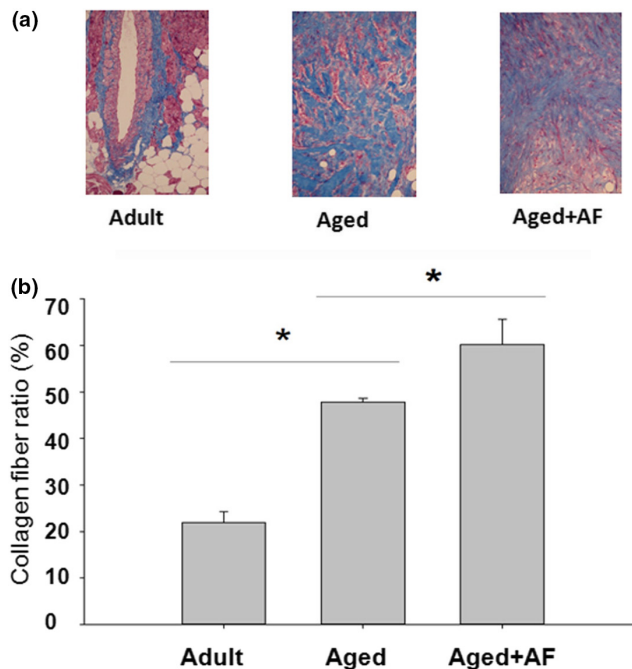

FIGURE 1 Fibrosis in the left atrium of each group. (a) Left atrial fibrosis (1 * 200 magnification); (b) Collagen fiber ratio among groups. *<0.05

increased in the elderly dog group and the AF elderly dog group. Compared with the elderly dog group, PVERPd and SNRT were significantly higher in the AF elderly dog group (Figure 3d). The above results indicate that aging prolongs the cardiac ERP and AF exacerbates cardiac ERP.

Subsequently, we conducted an ERP frequency adaptability analysis. The results showed that compared with the adult group, the frequency adaptability of LAA, CSd, LSPV, and LIPV ERP in the aged group was significantly reduced. In addition, the frequency adaptability of LAA, CSd, RAA, CSp, LSPV, LIPV, RSPV, and RIPV ERP of the aged AF dog group was significantly lower than that of the aged dog group (Figure 3d). The above results indicate that aging reduces the adaptability of heart ERP frequency, and AF again exacerbates this phenomenon.

3.4 | Aging and AF increases HCN2 and HCN4 expressions

We then separated the sinus node, left atrium, and pulmonary veins tissue and detected the expression of HCN2 and HCN4. The results showed that the protein and mRNA expression of HCN2 and HCN4 in the sinus node of aged dogs were significantly reduced. In the left atrium and pulmonary veins of aged dogs group, the protein and mRNA expression of HCN2 and HCN4 were significantly increased. Compared with the aged dog group, the protein and mRNA expression of HCN2 and HCN4 in the sinus node in the AF aged group were significantly reduced, and the protein and mRNA expression of HCN2
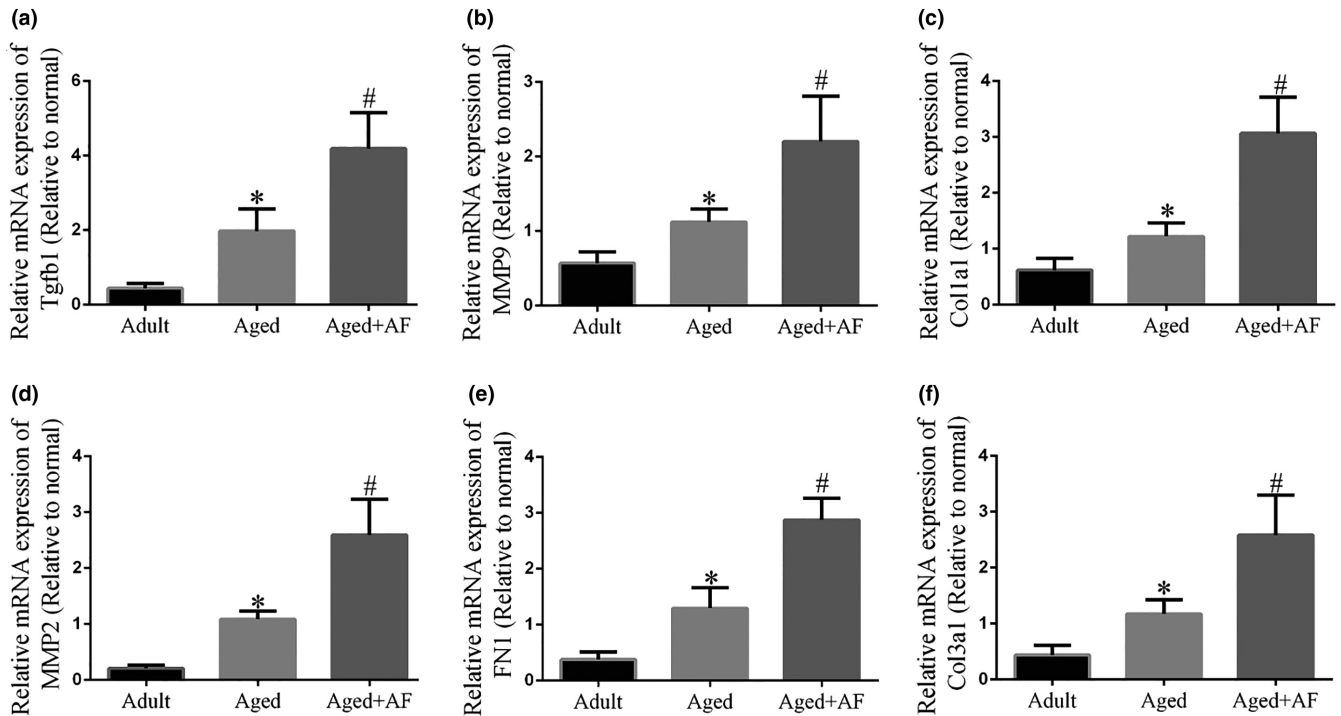
FIGURE 2 mRNA expression changes in the left atrium in the Aged group and the Aged +AF group. Fluorescence quantitative PCR was used to detect the expression of Tgfb1 (a), MMP9 (b), Col1a1 (c), MMP2 (d), FN1 (e), and Col3a1 (f) in the left atrium in dogs. * indicates a comparison with the Adult group. # indicates a comparison with the Aged group. $p < .05$
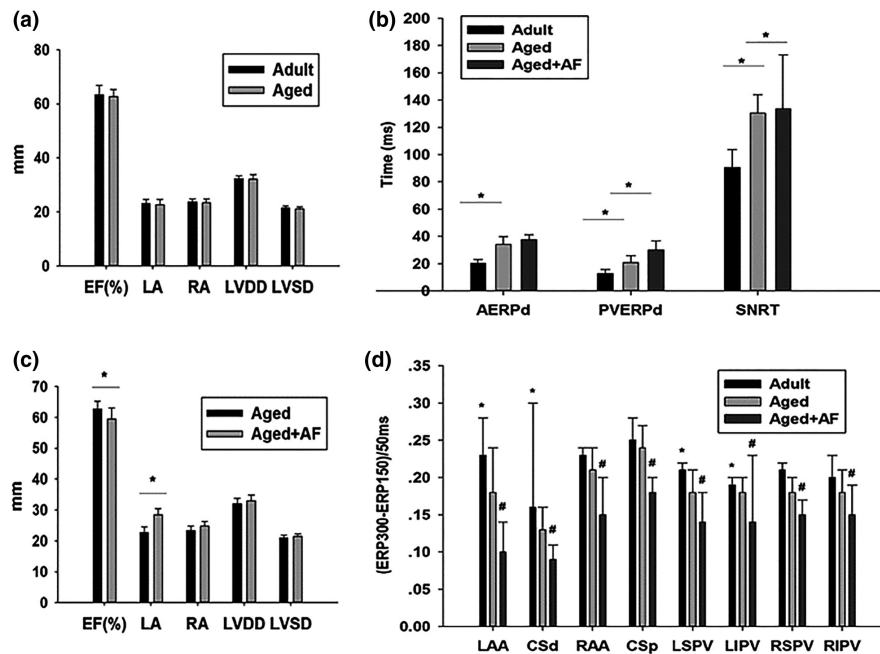
FIGURE 3 Result comparison between cardiac ultrasound testing and ERP at different sites. (a) Cardiac ultrasound was used to detect the changes of ejection fraction (EF), left atrium (LA), right atrium (RA), the end-diastolic diameter of left ventricle (LVDD), and the end-systolic diameter of left ventricle (LVSD) in the adult group and the Aged group. (b) Ultrasound was used to detect the changes of EF, LA, RA, LVDD, and LVSD in the Aged group and the Aged +AF group. * indicates Aged +AF group VS Aged group. $p < .05$. (c) An electrocardiogram was used to detect the changes in atrial effective refractory period dispersion, pulmonary vein effective refractory period dispersion, and correction of sinus node recovery time in the Adult group, the Aged group, and the Aged +AF group. * indicates a significant difference. $p < .05$. (d) The electrocardiogram was used to detect the adaptive changes in ERP frequency of the left atrial appendage, right atrial appendage, distal coronary vein, proximal coronary vein, left superior pulmonary vein, left inferior pulmonary vein, right superior pulmonary vein, and the right inferior pulmonary vein in the Adult group, the Aged group, and the Aged +AF group. * indicates the Adult group VS Aged group, # indicates the Aged +AF group VS Aged group. $p < .05$

and HCN4 in the left atrium and pulmonary veins were significantly increased (Figures 4a,b and 5a–c). The above results indicate that age and AF modulated the expression of HCN2 and HCN4 channels.

3.5 | Aging and AF change I_f density

The left atrial cardiomyocyte was isolated and the If current recorded in two groups (the aged AF group and the aged sinus rhythm group); the results showed that the If current can be specifically blocked by cesium chloride (Li et al., 2014). As shown in the present study, there was a significant difference in current amplitude between the aged AF group and the aged sinus rhythm group ($p ≤ .05$). There was no significant difference in cell membrane capacitances between the two groups ($p > .05$). However, the current densities of the three groups were $-25.2 ± 3.2$ pA/pF (the aged AF group), $-7.2 ± 2.2$ pA/pF (the aged sinus rhythm group), and $-2.9 ± 2.8$ pA/pF (the adult sinus rhythm group), respectively, and there was a significant difference between the aged AF group and the aged sinus rhythm group ($p ≤ .05$); (Figure 6).

## 3.6 | AF changes left atrium I_f activation kinetics in aged dogs

In the I_f activation kinetics, the activation thresholds were significantly higher in the aged sinus rhythm group than in the aged AF group. In the voltage-induced half activation, the activation thresholds were significantly higher in the aged sinus rhythm group than in the aged AF group. The I-V curve in the two groups showed that the current gradually increased with the hyperpolarization activation potential; this was most obvious in the aged AF group (Figures 7, 8 and Figure S1).

4 | DISCUSSION

In this study, aging was increased the degree of atrial fibrosis in dogs. Moreover, aging also significantly activates the HCN2/4 channels in the atria and pulmonary veins. AF exacerbates atrial fibrosis and changes in HCN2/4, K and calcium channels. The above results
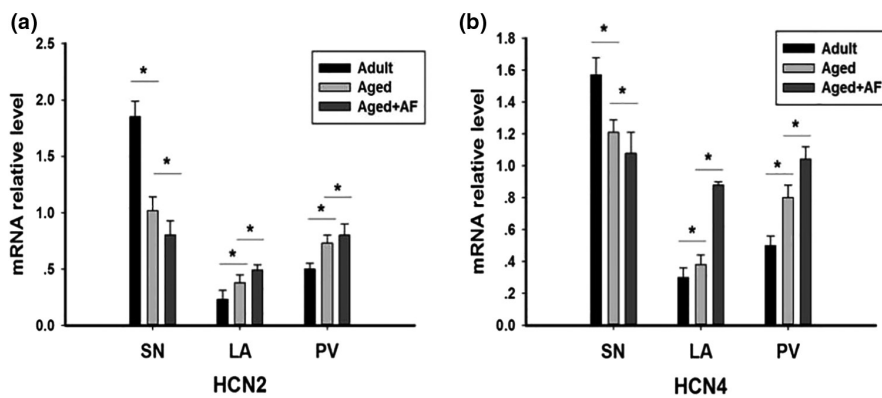
FIGURE 4 Changes in mRNA expression of HCN2 and HCN4 in the sinus node (SN), left atrium (LA), and pulmonary vein (PV). RT-PCR was used to detect the mRNA expression of HCN2 (a) and HCN4 (b) in SN, LA, and PV. $p < .05$
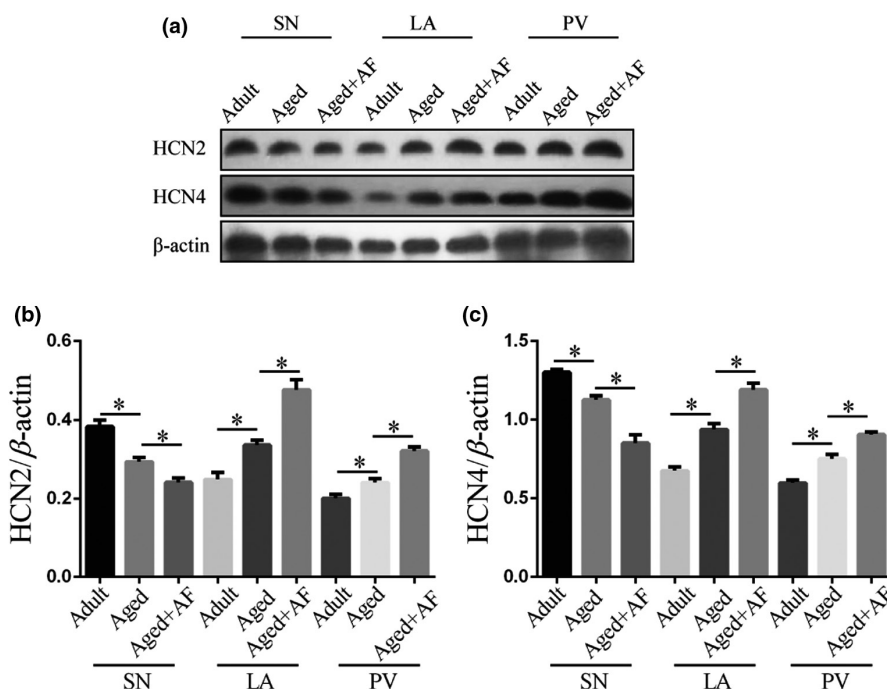
FIGURE 5 Changes in protein expression of HCN2 and HCN4 in the sinus node (SN), left atrium (LA), and pulmonary vein (PV). (a) Western blot was used to detect the protein expressions of HCN2 and HCN4 at different sites in the Atrial. Western blot was used to detect the protein expressions of HCN2 and HCN4 in SN, LA, and PV. (b) The protein bands of HCN2 and HCN4 were quantified, and GAPDH was used as the internal control to calculate the ratio. * <0.05

FIGURE 6 Current parameters of each group. (a) The current amplitudes of three groups. (b) The membrane capacitance of three groups. (c) Half activation voltage. (d) Current density of three groups. (e) Activation threshold potential. (f) Activation threshold potential. * indicates Aged +AF group VS Aged group. # indicates Adult group VS Aged group. $p < .05$
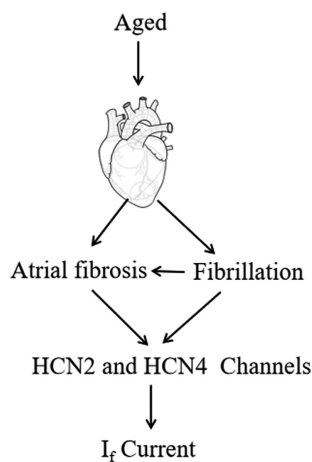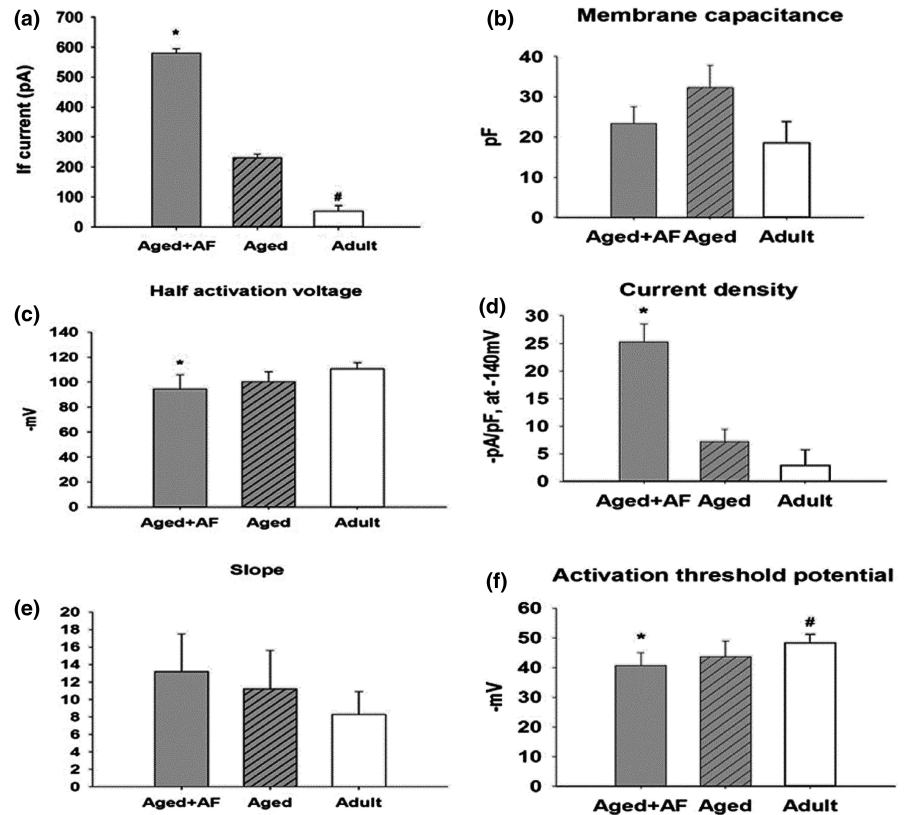
FIGURE 7 Aging will increase the degree of cardiac fibrosis and susceptibility to atrial fibrosis. Meanwhile, cardiac fibrosis and atrial fibrosis can change If Current through HCM2/4 Channels

suggest that aging exacerbates atrial fibrosis and affects HCN2/4, potassium, and calcium channels.

Atrial fibrillation is related to the structure, electricity, and contraction remodeling of the atrium (Nattel, 2017). The occurrence and development of atrial fibrosis is a sign of structural AF remodeling; it is considered the permanent basis of AF (Nattel, 2017). In the myocardium, fibrosis leads to many identifiable clinical features, including heart block, bundle branch block, left ventricular dysfunction, anisotropy, AF, ventricular arrhythmia,

systolic and diastolic dysfunction, heart failure, and cardiogenic death (Sohns & Marrouche, 2020). Therefore, studying the factors contributing to AF as well as its underlying mechanisms is important. In this study, the increase in the dogs' age was also accompanied by an increase in cardiac fibrous collagen deposition. In addition, the expression of fibrin markers in the atria increased significantly. These results suggest that age is an important risk factor for atrial fibrosis.

Previous studies have suggested that the atrial function suffers with age, where some conditions, such as prolonged action potential in cardiomyocytes, decrease in the platform period, increase in ERP dispersion, and decrease in wavefront conduction velocity, contribute to the development of AF (Kojodjojo et al., 2006). Xu et al. found that the electrophysiological characteristics of the atria and pulmonary veins also changed with age, with both an increase in dispersion and prolongation of the P wave and ERP (Xu et al., 2013). In addition, Dun et al. reported that the atrial myocyte membrane I_{to} increased with age (Verkerk & Wilders, 2015).

In the present study, a pacemaker was used to construct an AF model. It was found that AF induction in the atrium was more likely in the aged dogs. This may be due to atrial fibrosis changing the atrial structure. In addition, the occurrence of AF exacerbates the severeness of atrial fibrosis.

In order to further study how age affects AF occurrence, changes in atrial ion channels were subsequently monitored. The results showed that the protein and mRNA expressions of the HCN channel increased in the atria and pulmonary veins but decreased in the sinus node.
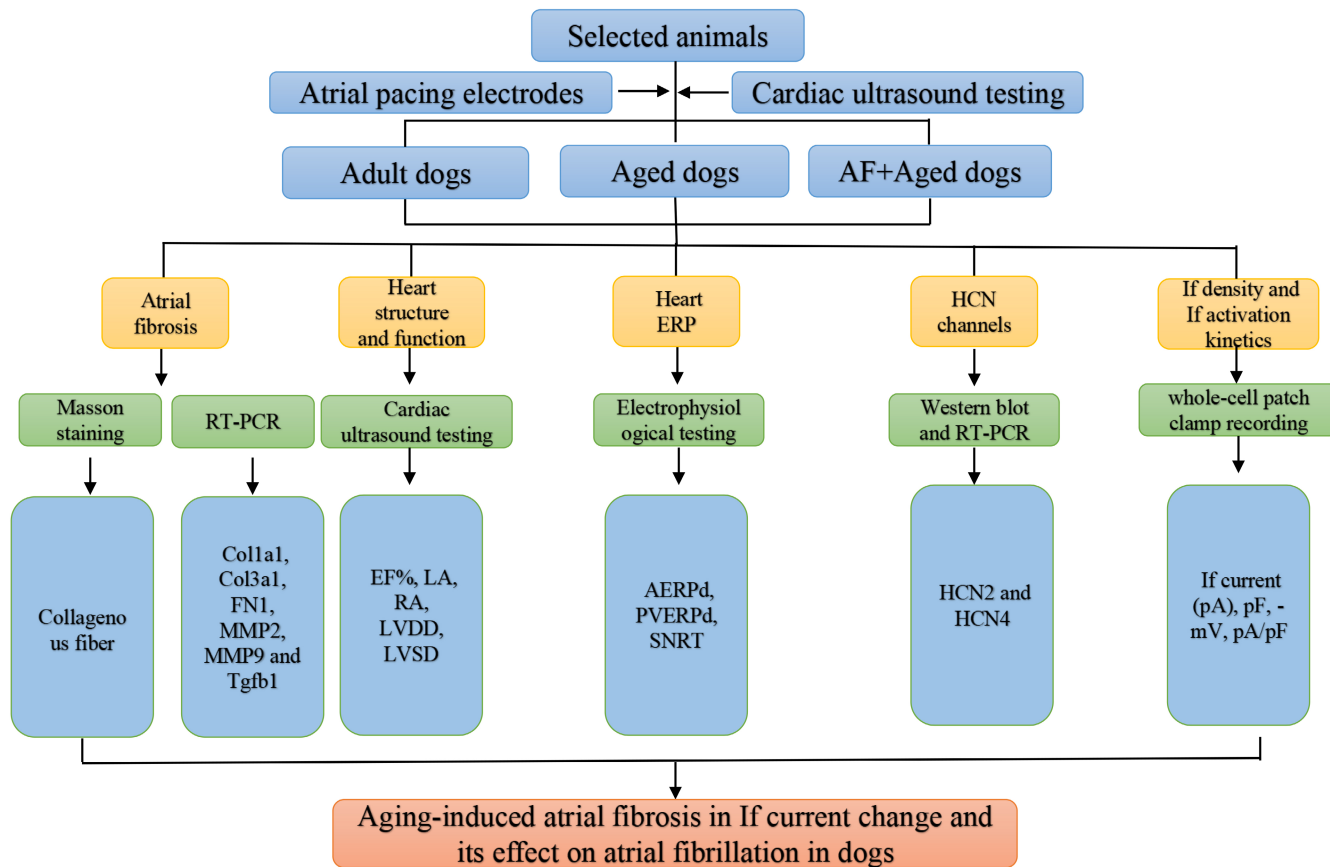
FIGURE 8 Flow chart (TOC Graphic)

Studies have shown that HCN channels play an important role in heart rhythm regulation (He et al., 2019) and that a lack of HCN2 and HCN4 can cause sinus dysfunction in mice (He et al., 2019). Overexpression of HCN2 and HCN4 channels will prolong the repolarization of ventricular action potentials, thereby increasing the possibility of arrhythmia (Herrmann et al., 2007). In addition, the potassium and calcium channel gene expressions are significantly reduced; these two channels have also been confirmed in a study on cardiac pacing function (Whitaker et al., 2007). These results indicate that age may potentially induce AF through changes in HCN1/2, potassium, and calcium channels.

The I_f current, a mixture of the sodium and potassium inward current, is mainly detected in the sinus node and is activated during depolarization; this is related to the pacing activity of the sinus node. The electrophysiological test results showed that the cardiomyocytes in the aged AF group demonstrated the highest I_f current frequency, followed by the aged sinus rhythm group and the adult sinus rhythm group; this is consistent with the results of the previous study (Wang et al., 2020). Compared with the sinus rhythm group, the I_f current detected in the atrial myocardium was increased in the aged AF group; this supports the notion that the I_f current is involved in the development of AF.

The I_f current in atrial cardiomyocytes is likely to become an ectopic pacemaker, accompanying the degeneration of sinus node function. An ectopic pacemaker provides an electrical basis for AF, whereas AF can intensify this electrical remodeling, thus leading to a worsening in AF. The I_f current was also increased in the aged sinus rhythm group compared with the adult group, indicating heart degeneration in aged dogs. The I_f current density also changed: the I_f current was identified mainly in the sinus node in adults and gradually showed a shift toward the working myocardium.

Taken together, our findings suggest that aging exacerbates atrial fibrosis and affects HCN2/4, potassium, and calcium channels. Moreover, AF also significantly increased the degree of atrial fibrosis.

CONFLICT OF INTEREST

The authors declare that they have no competing interests.

ETHICAL APPROVAL

The study protocol was approved by the ethics committee of the First Affiliated Hospital of Xinjiang Medical University (NO. IACUC201902-k05), and the guidelines for animal experiments were issued by the First Affiliated Hospital of Xinjiang Medical University were followed strictly in animal care and feeding procedures.

ORCID

Yao-Dong Li 🄳 https://orcid.org/0000-0003-3429-0985

REFERENCES

Babür Güler, G., Karaahmet, T., & Tigen, K. (2011). Myocardial fibrosis detected by cardiac magnetic resonance imaging in heart failure: Impact on remodeling, diastolic function and BNP levels. *Anadolu Kardiyoloji Dergisi*, 11(1), 71–76. https://doi.org/10.5152/akd.2011.013

Benarroch, E. E. (2013). HCN channels: Function and clinical implications. *Neurology*, 80(3), 304–310. https://doi.org/10.1212/WNL.0b013e31827dec42

Cremer, A., Lainé, M., Papaioannou, G., Yeim, S., & Gosse, P. (2015). Increased arterial stiffness is an independent predictor of atrial fibrillation in hypertensive patients. *Journal of Hypertension*, 33(10), 2150–2155. https://doi.org/10.1097/HJH.0000000000000652

Espeland, T., Lunde, I. G., H Amundsen, B., Gullestad, L., Aakhus, S. (2018). *Myocardial fibrosis. Tidsskr Nor Laegeforen*. 138(16). English, Norwegian.

Gyöngyösi, M., Winkler, J., Ramos, I., Do, Q. T., Firat, H., McDonald, K., González, A., Thum, T., Díez, J., Jaisser, F., Pizard, A., & Zannad, F. (2017). Myocardial fibrosis: Biomedical research from bench to bedside. *European Journal of Heart Failure*, 19(2), 177–191. https://doi.org/10.1002/ejhf.696

He, J. T., Li, X. Y., Zhao, X., & Liu, X. (2019). Hyperpolarization-activated and cyclic nucleotide-gated channel proteins as emerging new targets in neuropathic pain. *Reviews in the Neurosciences*, 30(6), 639–649. https://doi.org/10.1515/revneuro-2018-0094

Herrmann, S., Stieber, J., & Ludwig, A. (2007). Pathophysiology of HCN channels. *Pflugers Archiv. European Journal of Physiology*, 454(4), 517–522. https://doi.org/10.1007/s00424-007-0224-4

Hirosawa, K., Sekiguchi, M., Kasanuki, H., Kimata, S., Kaneko, N., Nakamura, K., Aosaki, M., Takahashi, S., & Kondo, M. (1987). Natural history of atrial fibrillation. *Heart and Vessels Supplement*, 2, 14–23.

Jiang, S., Li, T., Yang, Z., Yi, W., Di, S., Sun, Y., Wang, D., & Yang, Y. (2017). AMPK orchestrates an elaborate cascade protecting tissue from fibrosis and aging. *Ageing Research Reviews*, 38, 18–27. https://doi.org/10.1016/j.arr.2017.07.001

Kirchhof, P., Benussi, S., Kotecha, D., Ahlsson, A., Atar, D., Casadei, B., Castellá, M., Diener, H.–C., Heidbuchel, H., Hendriks, J., Hindricks, G., Manolis, A. S., Oldgren, J., Alexandru Popescu, B., Schotten, U., Van Putte, B., & Vardas, P. (2017). 2016 ESC guidelines for the management of atrial fibrillation developed in collaboration with EACTS. *Revista Española De Cardiología (English Edition)*, 70, 50. https://doi.org/10.1016/j.rec.2016.11.033

Kojodjojo, P., Kanagaratnam, P., Markides, V., Davies, D. W., & Peters, N. (2006). Age-related changes in human left and right atrial conduction. *Journal of Cardiovascular Electrophysiology*, 17, 120–127. https://doi.org/10.1111/j.1540-8167.2005.00293.x

Li, H., Zhou, Y., Jiang, B., Zhao, X., Li, X., Yang, X., & Jiang, W. (2014). Dual effects of amiodarone on pacemaker currents in hypertrophied ventricular myocytes isolated from spontaneously hypertensive rats. *Clinical and Experimental Pharmacology and Physiology*, 41(9), 698–707. https://doi.org/10.1111/1440-1681.12264

Love, S., & Miners, J. S. (2016). Cerebrovascular disease in ageing and Alzheimer's disease. *Acta Neuropathologica*, 131(5), 645–658. https://doi.org/10.1007/s00401-015-1522-0

Nattel, S. (2017). Molecular and cellular mechanisms of atrial fibrosis in atrial fibrillation. *JACC: Clinical Electrophysiology*, 3(5), 425–435. https://doi.org/10.1016/j.jacep.2017.03.002

Oldgren, J., Healey, J. S., Ezekowitz, M., Commerford, P., Avezum, A., Pais, P., Zhu, J., Jansky, P., Sigamani, A., Morillo, C. A., Liu, L., Damasceno, A., Grinvalds, A., Nakamya, J., Reilly, P. A., Keltai, K., Van Gelder, I. C., Yusufali, A. H., Watanabe, E., ... Yusuf, S. (2014). Variations in cause and management of atrial fibrillation in a prospective registry of 15,400 emergency department patients in 46 countries: The RE-LY atrial fibrillation registry. *Circulation*, 129, 1568–1576. https://doi.org/10.1161/CIRCULATIONAHA.113.005451

Rivolta, I., Binda, A., Masi, A., & DiFrancesco, J. C. (2020). Cardiac and neuronal HCN channelopathies. *Pflugers Archiv. European Journal of Physiology*, 472(7), 931–951. https://doi.org/10.1007/s00424-020-02384-3

Sohns, C., & Marrouche, N. F. (2020). Atrial fibrillation and cardiac fibrosis. *European Heart Journal*, 41(10), 1123–1131. https://doi.org/10.1093/eurheartj/ehz786

Thihalolipavan, S., & Morin, D. P. (2015). Atrial fibrillation and heart failure: Update 2015. *Progress in Cardiovascular Diseases*, 58, 126–135. https://doi.org/10.1016/j.pcad.2015.07.004

Verkerk, A. O., & Wilders, R. (2015). Pacemaker activity of the human sinoatrial node: An update on the effects of mutations in HCN4 on the hyperpolarization-activated current. *International Journal of Molecular Sciences*, 16, 3071–3094. https://doi.org/10.3390/ijms16023071

Wang, Z., Tapa, S., Francis Stuart, S. D., Wang, L., Bossuyt, J., Delisle, B. P., & Ripplinger, C. M. (2020). Aging disrupts normal time-of-day variation in cardiac electrophysiology. *Circulation: Arrhythmia and Electrophysiology*, 13(9), e008093. https://doi.org/10.1161/CIRCEP.119.008093

Whitaker, G. M., Angoli, D., Nazzari, H., Shigemoto, R., & Accili, E. A. (2007). HCN2 and HCN4 isoforms self-assemble and co-assemble with equal preference to form functional pacemaker channels. *Journal of Biological Chemistry*, 282(31), 22900–22909. https://doi.org/10.1074/jbc.M610978200

Xu, G.-J., Gan, T.-Y., Tang, B.-P., Chen, Z.-H., Jiang, T., Song, J.-G., Guo, X., & Li, J. (2013). Age-related changes in cellular electrophysiology and calcium handling for atrial fibrillation. *Journal of Cellular and Molecular Medicine*, 17, 1109–1118. https://doi.org/10.1111/jcmm.12084

Zoni-Berisso, M., Lercari, F., Carazza, T., & Domenicucci, S. (2014). Epidemiology of atrial fibrillation: European perspective. *Clinical Epidemiology*, 6, 213–220. https://doi.org/10.2147/CLEP.S47385

SUPPORTING INFORMATION

Additional supporting information may be found in the online version of the article at the publisher's website.